The effect of varying loading directions and loading levels on crack growth at 2D- and 3D-mixed-mode-loadings

A. Eberlein, H.A. Richard

Institue of Applied Mechanics, University of Paderborn, Pohlweg 47-49, 33098 Paderborn, Germany
eberlein@fam.upb.de

ABSTRACT. While product's operation the loading situation commonly changes. The local loading situation on an existing crack then can shift to a combined loading, composed of mode I, mode II and mode III, and consequently influence the product's durability significantly. This influence on further fatigue crack growth and structures' failure can be positive or negative. Present article describes and discusses the effect of varying loading directions from mode I- to 2D-mixed-mode-loading as well as from mode I- to mixed-mode I + III-loading. Moreover, experiments on varying loading levels are performed by interspersing mixed-mode block loads in cyclic mode I base load, cyclic mode II base load as well as in cyclic mode III base load.

KEYWORDS. 3D-mixed-mode; Loading directions; Loading levels; CTSR-specimen; 3D-fatigue crack growth.

INTRODUCTION

P arts in many technical applications often are subjected to variable cyclic loading. While service life these products due to transportation, assemblage, site of operating as well as in use experience time-dependent loadings, so-called service loadings, which result from single over-/underloads, variable loading levels as well as changing loading directions. Thereby the crack growth can both accelerate and retard. Anyway, the fatigue crack growth is not only controlled by the current loading parameters ΔK and R-ratio, but also by the loading history. Due to the fact that different loading changes interact with each other during a service loading, the characterisation of the whole interaction effects on fatigue crack growth under variable loading amplitude are generally investigated separately by means of four different categories. Sander [1] classify these in single over-/underloads, over-/underload sequences, block loading and service loading. The experimental investigations in this contribution study the fatigue crack growth under variable loading amplitude by interspersing block loading into a constant baseline-level loading. Block loadings represent several succeeding overloads. Generally, block loadings are distinguished between high-low, low-high or the appropriate combination low-high-low sequences [2]. Within the block loadings the R-ratio can be different. Therefore block loadings can be classified in three types of low-high-low sequences, whereby always one characteristic parameter during the transition from one to the next block load is constant. The characteristic parameters are $K_{Bl,min} = $ const., $R = $ const. and $\Delta K_{Bl} = $ const. In this paper the block loading tests were performed with a constant R-ratio, as Fig. 1 shows.
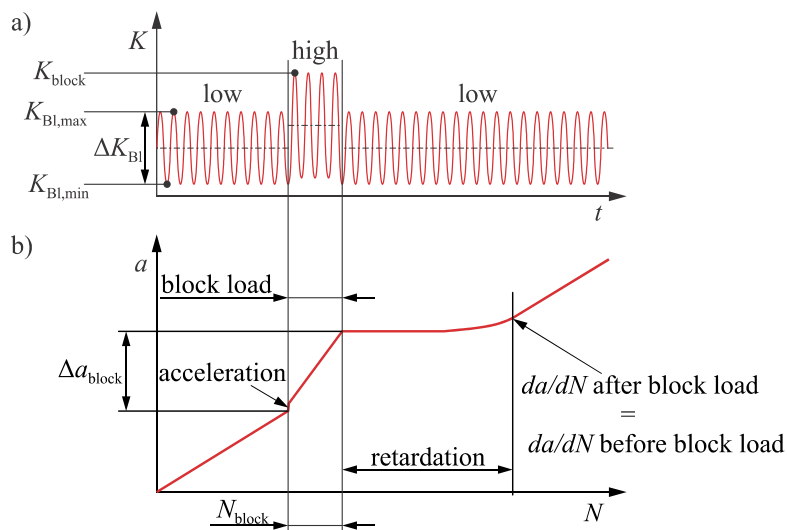
Figure 1: Crack retardation and acceleration while low-high-low block load sequence; (a) Parameters of a low-high-low block load sequence with constant R-ratio; (b) Schematic a-N-curve after a low-high-low block load sequence according to Richard and Sander [2].

Hereby the definition of characteristic variables can be extracted from Fig. 1 a). A crucial influence on component's durability has the level of the block loading. As within this experiments also mixed-mode-block loadings are interspersed, the level of the block loading is defined by the block loading ratio $R_{V,block}$ as follows:

$$R_{V,block} = \frac{K_{V,block}}{K_{Bl,max}} \tag{1}$$

$K_{V,block}$ is the maximum comparative stress intensity factor during the block loading and $K_{Bl,max}$ is the maximum stress intensity factor of the baseline-level loading. The maximum comparative stress intensity factor can be determined by:

$$K_{V,block} = \frac{K_{I,block}}{2} + \frac{1}{2} \cdot \sqrt{K_{I,block}^2 + 5.336 \cdot K_{II,block}^2 + 4 \cdot K_{III,block}^2} \tag{2}$$

Such a block loading test with a number of block cycles N_{block} causes after a short acceleration phase a higher crack growth rate during the block loading. After that a retardation phase of the crack growth follows, which continues till the crack, if able to propagate, reaches its crack growth rate $(da/dN)_{Bl}$ of the baseline-level loading before the block loading (shown in Fig. 1 b)). Apart from changing loading levels also changing in essential loading as well as changing loading directions can appear while product's operation. Consequently, a variation of the global loading can effect a locally changing of the crack fracture mode e. g. from pure mode I-loading to an in-plane mixed-mode- or a 3D-mixed-mode-loading situation.

CTSR-SPECIMEN AND LOADING DEVICE

The experimental tests were performed using the CTSR-specimen (*Compact-Tension-Shear-Rotation*-specimen) with the corresponding loading device developed by Schirmeisen [3] and can be also found in Eberlein [4]. Fig. 2 illustrates the specimen's geometry (Fig. 2 a)) and the adjustment of the fracture modes (mode I, mode II and mode III) by the loading angles *a* and *β* on the loading device.

The corresponding loading device basically consists of two sickles and two inboard so-called turrets, where the specimen is fixed. By varying the loading angle *a* in the range of 0° till 90° by 15°-steps the mode I-ratio to mode II respectively mode III is regulated. A mounting position of the loading device of *a* = 0° corresponds with a pure mode I-loading at the crack front of the CTSR-specimen, as in Fig. 2 b) illustrated. Mounting the loading device with the specimen in a position

of $a = 90°$ and varying the loading angle β by rotating the turrets in the range of 0° till 90° by 15°-steps the loading situation at the crack front of the specimen can be adjusted from pure mode II-loading to pure mode III-loading, as Fig. 2 b) shows. Are both loading angles in a range between 15° and 75° this concept enables investigating the crack growth under 3D-mixed-mode-loading conditions.

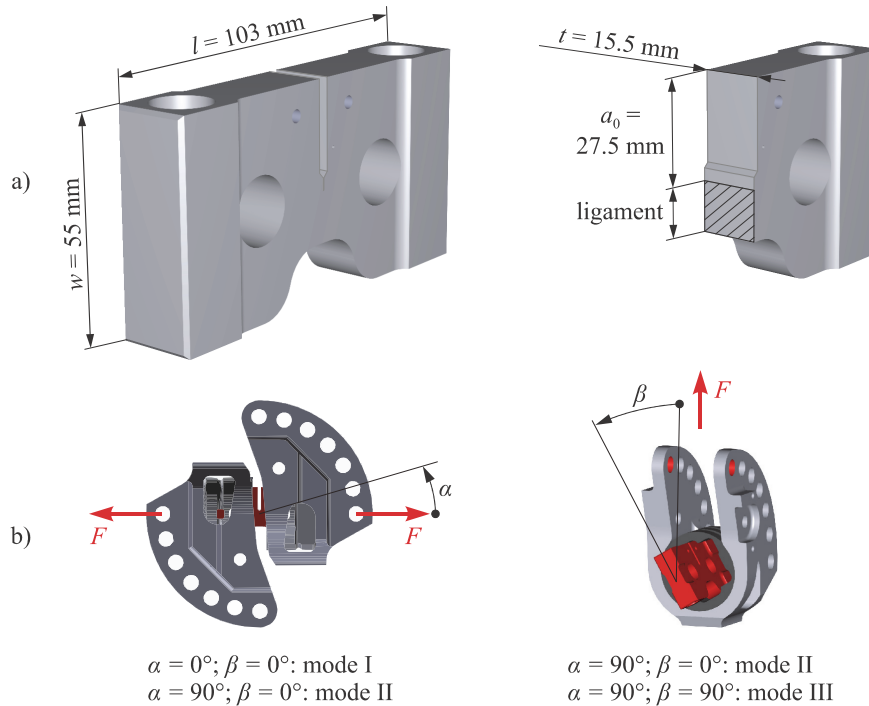Figure 2: CTSR-specimen and corresponding loading device. (a) Specimen's geometry and dimensions: length *l*, width *w*, initial crack length a_0, thickness *t* and ligament in sectional view; (b) Adjustment of loading angles *a* and *β* on loading device.

EXPERIMENTS

Within this contribution different series of crack growth experiments were performed. Therefor the CTSR-specimens were made from aluminium alloy 7075-T651. The different test series are described below in detail.

Series of experiments

In the first test series various in-plane mixed-mode-ratios with $\Delta K_I \neq 0$ and $\Delta K_{II} \neq 0$ respectively spatial mixed-mode-ratios with $\Delta K_I \neq 0$ and $\Delta K_{III} \neq 0$ by shifting the loading device are adjusted after a mode I-crack growth of $\Delta a = 3.5$ mm under constant cyclic stress intensity factor $\Delta K_I = $ const. After changing the loading direction the tests again start under constant cyclic loading force conditions $\Delta F = $ const., from which a cyclic comparative stress intensity factor ΔK_V results, which is equivalent to the cyclic stress intensity factor ΔK_I just before changing the loading direction. Thereby similar loading conditions before and after the mixed-mode-adjustment are given at the crack front.

The second test series investigate possible impacts of changing loading levels on crack growth by interspersed mixed-mode-block loads in mode I-, mode II- as well as in mode III-base loads. In mode I- and in mode II-base load the cyclic stress intensity factor is $\Delta K_{I,Bl} = \Delta K_{II,Bl} = 90$ MPa $\sqrt{\text{mm}}$. Whereas the level of mode III-base load is $\Delta K_{III,Bl} = 160$ MPa $\sqrt{\text{mm}}$. The R-ratio of the base load is 0.1. After a crack growth of $\Delta a = 2.0$ mm in the base loading the mixed-mode-block loads are interspersed for $N_{block} = 10,000$ cycles with a block loading ratio of $R_{V,block} = 2.0$ (cf. Eq. 1). Thereafter the loading direction is changed again to the base loading by shifting the loading device.

Varying loading directions with constant cyclic comparative stress intensity factor ΔK_V

Starting from a pure mode I-loading Fig. 3 shows the impacts on fatigue crack growth after changing loading directions from mode I-loading to mode I and mode II loading combinations. The region, where ΔK_V is nearly constant

85 MPa $\sqrt{mm}$ is encircled. With increasing mode II-part a growing crack growth retardation is noticeable. The crack kinks directly after changing loading direction in a new orientation and propagates significantly slower at K_{II}/K_{I}-ratios ≥ 0.99. The greatest effect in retardation resp. the greatest advantage in durability causes changing loading direction from pure mode I-loading to pure shear loading (mode II).
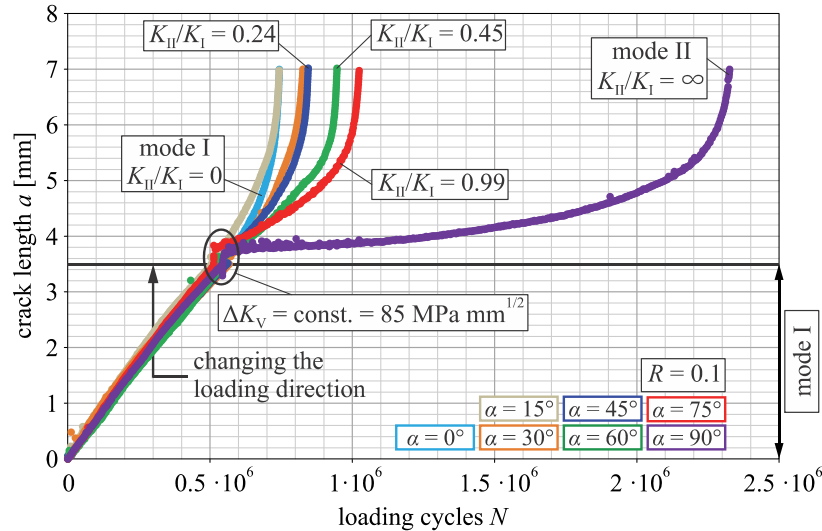

Figure 3: *a-N*-curves before and after change of mode I-mode II-loading direction.

Similar investigations on the impact of mode I-mode II-changing loading directions on an initial mode I-loading already were performed by Sander and Richard [5] and Richard et al. [6]. The findings herein agree with their results. However possible effects of changing loading directions on 3D-mixed-mode were not investigated therein. Therefore Fig. 4 illustrates the influence of mode I-mode III-changing loading directions on an initial mode I-loading. Due to the mode III-loading part hereby a significantly higher cyclic comparative stress intensity factor of $\Delta K_V = 140$ MPa $\sqrt{mm}$ was chosen, so that the crack still is able to propagate under pure mode III-loading. This high loading level explains the steep slope of the mode I-crack growth. Here the end crack length of $a = 7$ mm is reached after approximately $N = 70,000$ cycles by K_{III}/K_{I}-ratios < 0.57.
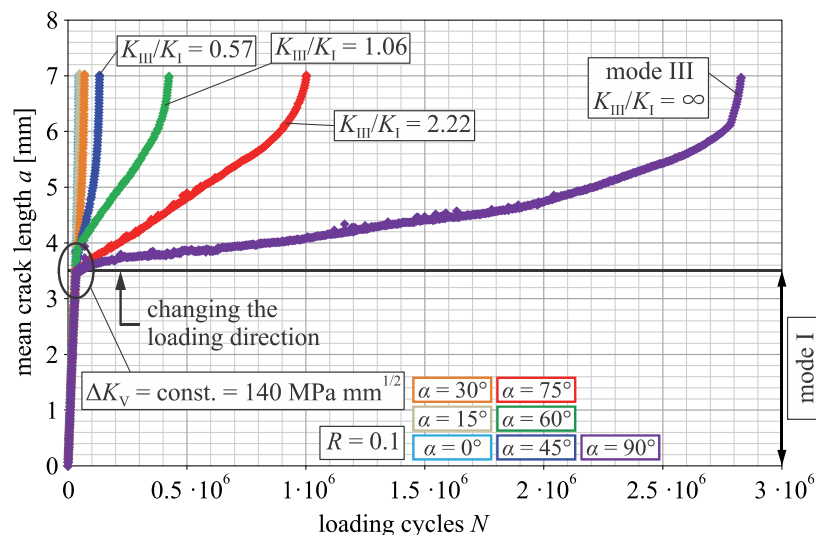

Figure 4: *a-N*-curves before and after change of mode I-mode III-loading direction.

Similar to the in-plane mixed-mode-changing loading directions the mode I-mode III-changing loading directions also show an increasing crack growth retardation with growing mode III-part. At the moment of changed loading direction the crack realigns by twisting out of its initial position. The crack growth process at mixed-mode-loadings in presence of

mode III-loading component is completely different to other combined loading conditions without mode III-part. Along the crack front several fatigue cracks initiate facetedly, so that each facet forms a new crack front. Fig. 5 presents typical fractured surfaces resulting from performed experiments depending on the mode III-part of the $K_{III}/(K_I + K_{III})$-ratio.
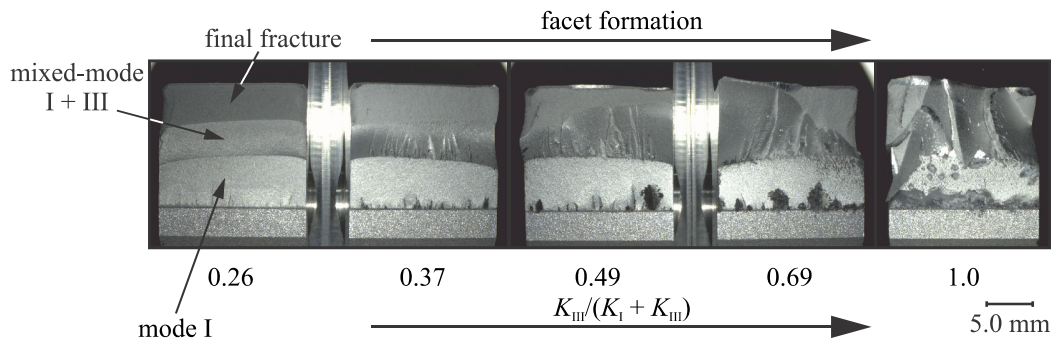

Figure 5: Facet formation depending on mode III-part.

Conspicuous within this experiments is that no facet formation occurs below a $K_{III}/(K_I + K_{III})$-ratio of 0.26. Many small and wispy facets start to create from a $K_{III}/(K_I + K_{III})$-ratio of 0.37 (that means $K_{III}/K_I = 0.57$) and coarsen their shape with increasing mode III-part obviously. The number of facets concurrently declines up to a few big facets as the fractured surface resulting from pure mode III-loading in Fig. 5 depicts. Concerning the crack deflection angles the changing loading directions show no unexpected impacts. Fig. 6 a) shows the measured crack kinking angle φ_0 compared to the hypothesis by Richard [7]. Hereby just the changing loading direction from pure mode I- to pure mode II-loading exhibits a ca. 10° lower crack kinking angle as the hypothesis predicts. The comparison of the crack twisting angle ψ_0 with the hypothesis by Richard [7] in Fig. 6 b) shows overall good accordance.
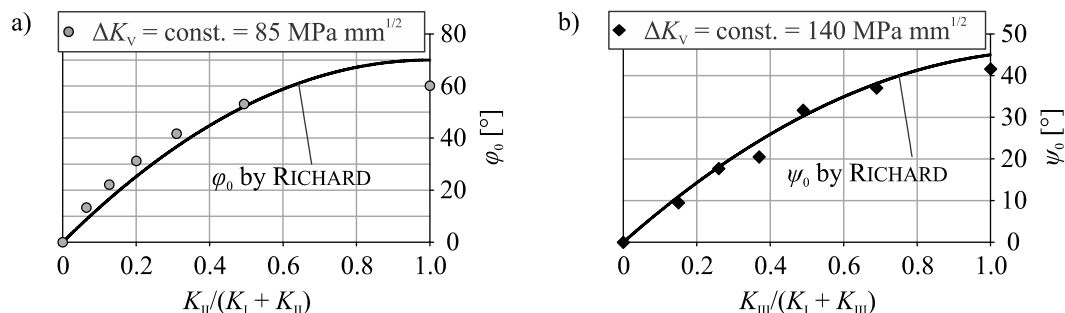

Figure 6: Crack deflection angles φ_0 and ψ_0 depending on the ratio of stress intensity factor. (a) Crack kinking angle φ_0 depending on $K_{II}/(K_I + K_{II})$; (b) Crack twisting angle ψ_0 depending on $K_{III}/(K_I + K_{III})$.

Influence of varying loading levels on mode I-, mode II- and mode III-crack growth
Different crack growth retardations due to mode I-, mode I-mode III- and mode III-block loads on mode I-base load are shown in Fig. 7. The K_{III}/K_I-ratios denoted in Fig. 7 are valid for the point of interspersing the block loads. In Fig. 7 it can be seen that the greatest crack growth retardation occurs by a pure mode I-block load. In this case the crack even arrests. Because even after 10^7 cycles a crack growth was not measured anymore.
To maintain the overview the x-axis is cut here at $N = 1.5 \cdot 10^6$ cycles. Due to the mode I-block load a bigger plastic zone at the crack front generates wherein residual compressive stresses form, which close the crack flanks. Moreover, the effect of retardation decreases with increasing mode III-part in order that a pure mode III-block load shows no influence on a crack growth in mode I-base load. This is affiliated to the displacement of the crack flanks. Under pure mode III-loading the biggest displacement of the crack flanks happens in z-direction and not as under mode I-loading in y-direction (perpendicular to the crack propagation). Accordingly, it can be assumed that a mode III-block load leads to twisting the plastic zone in z-direction so that a mode III-block load does not influence a crack in mode I-base load. Sander and Richard [8] already showed for in-plane mixed-mode-block loads that the plastic zone turns due to a shear loading (mode II). Moreover, the retardation effect on a mode I-loaded crack thereby decreases or is not existing anymore. The impacts

of interspersed mode I-mode II-block loads on mode II-base load are shown in Fig. 8. Here a pure mode II-block load causes the greatest retardation effect on the crack growth in mode II-base load.
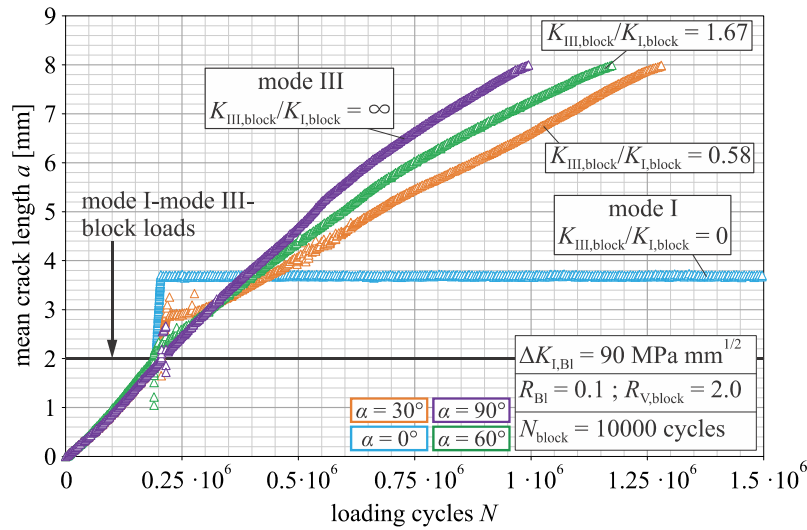

Figure 7: Crack growth retardation due to interspersed mode I-mode III-block loads in mode I-base load.
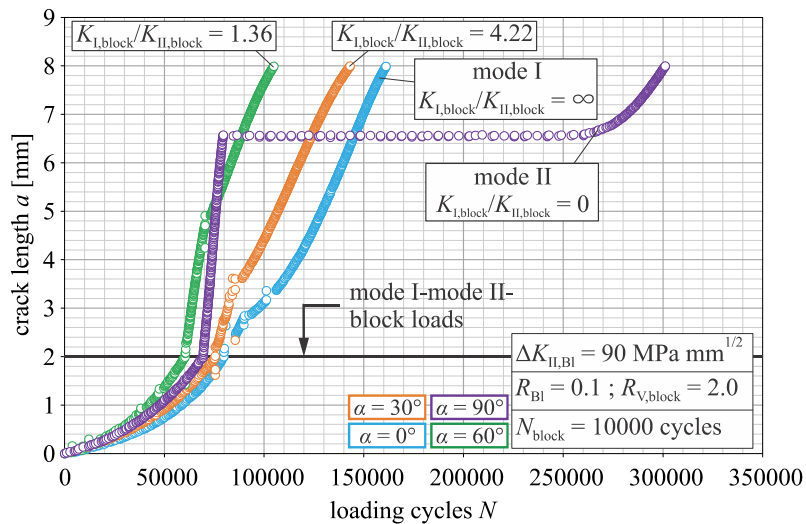

Figure 8: Crack growth retardation due to interspersed mode I-mode II-block loads in mode II-base load.

Indeed, the displacement according to amount of the crack flanks increases in y-direction with increasing mode I-component of the mode I-mode-II-block load and enlarges the plastic zone at the crack front, but the residual compressive stresses does not retard the crack growth in mode II-base load. The reason for that is the displacement of the crack flanks in mode II-base load, which takes place parallel to the crack growth direction.

In comparison to the crack growth in mode I- and mode II-base load the crack growth in mode III-base load due to interspersed mode I-, mode III- as well as mode I-mode III-block load combinations shows varyingly strong retardations (see Fig. 9). Indeed, it can be observed that the retardation effect decreases with increasing K_I/K_{III}-ratio, nevertheless the influence of the mode I-component in the mode I-mode III-block loads on a mode III-loaded crack is still existing. A part of typical fractured surfaces developed within the experiments are presented in Fig. 10. The fractured surfaces show for interspersed mode I-mode II-block loads in mode II-base load expected characteristics. Due to a pure mode I-block load a significant step on the fractured surface arises (Fig. 10 a)). Concerning the crack growth direction a crack kinking angle φ_0 of ca. 63° was measured before as well as after interspersing the block load. The fractured surfaces resulting from interspersed mode I-mode III-block loads in mode III-base load, shown in Fig. 10 b), reveal several facets and are relatively jagged. In conclusion, it can be registered that the greatest retardation effects respectively the greatest advantages

in durability are obtained, if the crack loading mode of the block loading coincides with the crack loading mode of the base loading.
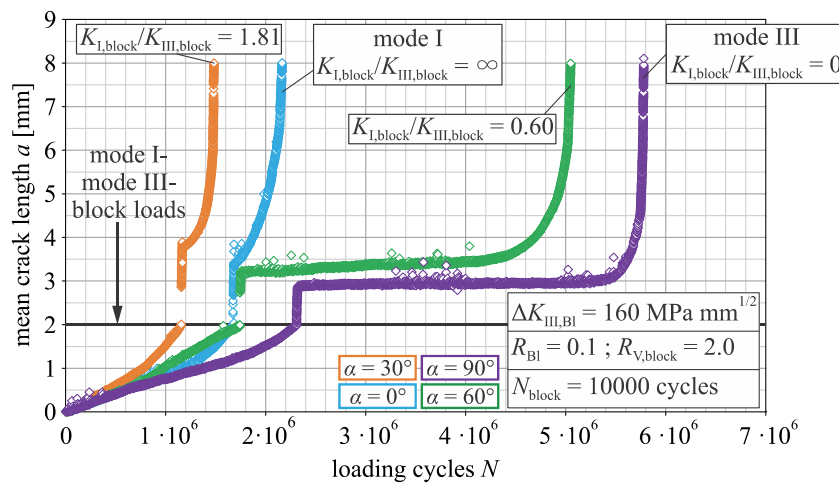

Figure 9: Crack growth retardation due to interspersed mode I-mode III-block loads in mode III-base load
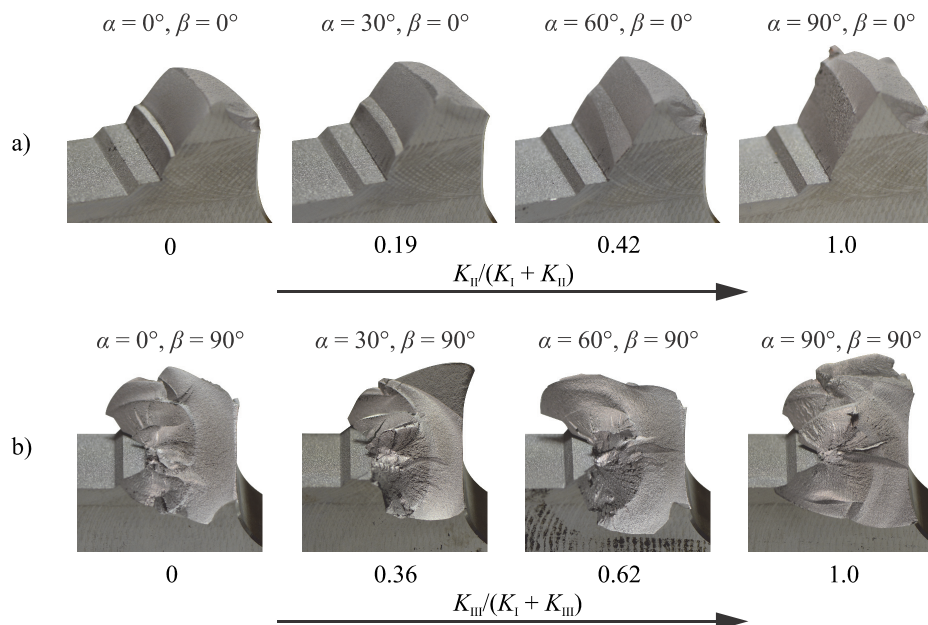

Figure 10: Typical fractured surfaces by varying loading levels. (a) Mode I-mode II-block loads in mode II-base load; (b) Mode I-mode III-block loads in mode III-base load.

REFERENCES

[1] Sander, M., Einfluss variabler Belastung auf das Ermüdungsrisswachstum in Bauteilen und Strukturen. Fortschritt-Berichte VDI: Reihe 18, Mechanik, Bruchmechanik, Band 287, VDI-Verlag, Düsseldorf, (2003).

[2] Richard, H. A., Sander, M., Ermüdungsrisse. 3. Auflage, Vieweg+Teubner, Wiesbaden, (2012).

[3] Schirmeisen, N.-H., Risswachstum unter 3D-Mixed-Mode-Beanspruchung. Fortschritt-Berichte VDI: Reihe 18, Mechanik, Bruchmechanik, Band 335, VDI-Verlag, Düsseldorf, (2012).

[4] Eberlein, A., Einfluss von Mixed-Mode-Beanspruchung auf das Ermüdungsrisswachstum in Bauteilen und Strukturen. Fortschritt-Berichte VDI: Reihe 18, Mechanik, Bruchmechanik, Band 344, VDI-Verlag, Düsseldorf, (2016).

[5] Sander, M., Richard, H. A., Effects of block loading and mixed mode loading on the fatigue crack growth, In: Proceedings of the 8th International Fatigue Congress (Fatigue 2002), Blom A. F. (Ed.), Stockholm, Sweden, (2002) 2895-2902.

[6] Richard, H. A., Linnig, W., Henn, K., Fatigue crack propagation under combined loading. Forensic Engineering 3 (1991) 99-109.

[7] Richard, H. A., Fulland, M., Sander, M., Theoretical crack path prediction. Fat. & Frac. of Eng. Mat. & Struc., 28 (2005) 3-12.

[8] Sander, M., Richard, H. A., Finite element analysis of fatigue crack growth with interspersed mode I and mixed mode overloads. International Journal of Fatigue, 28 (2005) 905-913.